Materials Today Bio 31 (2025) 101490

Contents lists available at ScienceDirect

Materials Today Bio

journal homepage: www.journals.elsevier.com/materials-today-bio

Electrostimulation combined with biodegradable electroactive oriented nanofiber polycaprolactone/gelatin/carbon nanotube to accelerate wound healing

Weizhi Chen [a,b,1], Yiliu Wei [a,1], Jing Chang [c,d,e,1], Yuwen Hui [c,d,e], Junchen Ye [a], Geng Weng [f], Ming Li [c,d,e,*], Yanhua Wang [c,d,g,**], Qiaoyi Wu [a,b,***]

[a] Department of Trauma Center and Emergency Surgery, The First Affiliated Hospital of Fujian Medical University, Fuzhou, China
[b] Department of Trauma Center & Emergency Surgery, National Regional Medical Center, Binhai Campus of the First Affiliated Hospital, Fujian Medical University, Fuzhou, China
[c] Key Laboratory of Trauma and Neural Regeneration, Ministry of Education, Peking University, Beijing, China
[d] National Center for Trauma Medicine, Beijing, China
[e] Trauma Medicine Center, Peking University People's Hospital, Beijing, China
[f] Fujian Institute for Food and Drug Quality Control, Fuzhou, China
[g] Department of Orthopedics and Trauma, Peking University People's Hospital, Beijing, 100044, China

ARTICLE INFO

Keywords:
Exogenous electrical stimulation
Electroactive
Oriented nanofiber
Wound healing

ABSTRACT

Wound healing is a complex but precise physiological process. Howener, existing treatments are often difficult to meet the needs of different wound healing. With the background that exogenous electrical stimulation (ES) has been proven to be effective in regulating cell behavior, we constructed a electroactive wound dressing derived from carbon nanotubes (CNT) by electrospinning technology. The scaffold has a moderate hydrophilicity, which benefits to collecting of effusion, adhering to the wound site, and safely removing. Furthermore, the oriented structure has the potential to promote cell oriented growth, while the coupling of endogenous electric field (EFs) and ES could effectively regulate the phenotype of macrophages and reshape the immune microenvironment. At the same time, the active electrical stimulation promotes the secretion of active factors and the proliferation and migration of fibroblasts and endothelial cells. In vivo assays further confirm that PCL/GE/CNT combined ES strategy can significantly inhibit the early inflammatory response, while promoting vascular regeneration and collagen deposition. RNA sequencing analysis is used to reveal the mechanism at the molecular level. Overall, this study employed a composite strategy of combining CNT with moderately hydrophilic biocompatible nanofibers to achieve ES delivery simply and effectively, significantly improving tissue engineering outcomes. This innovative strategy provides a feasible approach for efficient wound repair, and provides an important experimental basis and theoretical guidance for future development in the field of skin tissue engineering.

1. Introduction

Wound healing has become one of the major health challenges around the world, with approximately 14 million people suffering from wounds each year [1]. Normal wound healing is a dynamic and complex multi-stage process, which includes four stages of hemostasis, inflammation, cell proliferation and tissue regeneration, and involves complex coordinated interactions between growth factors, cytokines, chemokines and various cells [2]. Current wound treatment include debridement and dressing change, negative pressure closed drainage, autologous skin transplantation and artificial skin, etc. [3,4], but due to the complexity of the wound healing process, these traditional methods

* Corresponding author. Key Laboratory of Trauma and Neural Regeneration, Ministry of Education, Peking University, Beijing, China.
** Corresponding author. National Center for Trauma Medicine, Beijing, China.
*** Corresponding author. Department of Trauma Center and Emergency Surgery, The First Affiliated Hospital of Fujian Medical University, Fuzhou, China.
E-mail addresses: liming_ort@bjmu.edu.cn (M. Li), 94719599@qq.com (Y. Wang), qywu@mail.fjmu.edu.cn (Q. Wu).
[1] These authors contributed equally to this work.

https://doi.org/10.1016/j.mtbio.2025.101490
Received 27 October 2024; Received in revised form 10 January 2025; Accepted 12 January 2025
Available online 13 January 2025

cannot meet the current needs. In recent years, multifunctional wound dressings have shown considerable potential in the field of wound healing. However, most dressings used for wound healing focus only on improving tissue perfusion and reducing infection, and are rarely involved in actively regulating endogenous cellular behavior. Therefore, it is very necessary to develop a new wound treatment method that can promote the cell regeneration behavior at the wound site and actively promote wound healing and tissue regeneration.

Wound healing is a delicate and complex process that requires multiple cells, molecules, and signaling pathways to be closely linked to effectively achieve tissue repair [5]. During the process, the endogenous electrical signal plays a crucial role in regulation. It has been found that after skin injury, the wound site generates endogenous electric field (EFs) that points to the center of the wound [6]. This EFs usually has the ability to guide the migration of cells (e.g., fibroblasts, endothelial cells, and macrophages) towards the wound and has a significant impact on wound re-epithelialization [6]. Studies have shown that in the early stage of inflammation, EFs can accelerate the aggregation of immune cells and cytokines, and indirectly play an antibacterial role [7]. However, in the late stage of inflammation, EFs can appropriately reduce the aggregation of immune cells and cytokines to avoid an overly strong inflammatory response [8]. At the same time, EFs can improve blood circulation by activating vascular response and stimulating endothelial cell migration [9]. It can also promote wound re-epithelialization by promoting granulation tissue formation and collagen synthesis, as well as keratinocyte and fibroblast migration [10,11]. Inspired by the effect of EFs on wound sites, exogenous electrical stimulation (ES) has been used to treat trauma, mainly to mimic and enhance the effect of endogenous EFs [12]. However, the use of exogenous electrical stimulation faces the challenge of lacking materials with strong electrical conductivity and good biocompatibility.

In recent years, some conductive materials, such as polypyrrole (PPY), polyaniline (PANI), poly-phenylenevinylene (PPV) and carbon nanotubes (CNT), have received much attention due to their unique electrical activity [13]. Among them, CNT has strong mechanical properties, electrical conductivity and high biosafety performance, and is relatively easy to manufacture and realize functionalization. At present, many researches have been conducted to prepare conductive scaffolds for tissue damage repair by using CNT [14,15]. Among them, the PCL/GE oriented fiber scaffold prepared by electrospinning technology has been included in our consideration because of its unique advantages. Polycaprolactone (PCL) is an FDA-approved biodegradable material with good mechanical properties and biosafety [16]. However, the application of PCL in tissue engineering has significant limitations, mainly because of its hydrophobic surface properties, less bioactive ligands and long degradation time [17]. To overcome these limitations, PCL is often mixed with natural hydrophilic polymers with chemically reactive surfaces, such as gelatin, chitosan and alginate, to improve the surface structure and the cell affinity, and regulate the degradation process. By improving the mechanical strength of the structure and promoting cell adhesion and proliferation, PCL/GE composite scaffolds can better meet the needs of different stages of wound healing [18].

In addition, PCL/GE scaffolds combine the hydrophobicity of PCL and the hydrophilicity of GE, and this dual characteristic fiber membrane is of great significance for optimizing the performance of wound dressings and promoting wound healing. Moderate hygroscopicity helps keep wounds clean and promotes clotting, while the hydrophilicity of gelatin provides a good environment for cell proliferation [19]. At the same time, the hydrophobic surface of PCL can effectively prevent the intrusion of external fluids, helping to maintain a stable microenvironment around the wound [19].

Based on the above considerations, this study first used CNT as a conductive medium, and successfully prepared a multifunctional electroactive dressing, namely PCL/GE/CNT fiber scaffold. Subsequently, this multifunctional electroactive scaffold was used in combination with ES therapy to improve the rate of wound healing. We detailed demonstrated the preparation process of the scaffold and its application (Scheme 1) through a schematic diagram, and evaluated its properties such as hydrophilicity and electrical conductivity in detail. Furthermore, the study performed cell experiments in vitro and evaluated its biocompatibility in vivo using rat full layer skin defect models, while further investigating the ability of the dressings to promote skin tissue healing. Gene expression differences were detected by RNA sequencing analysis, which provides important clues to reveal the molecular mechanism of the electroactive scaffold in promoting skin healing. These detailed experiments and analyses provide key experimental basis and theoretical guidance for future research and application in the field of skin tissue engineering.

2. Materials and methods

2.1. The preparation of materials

PCL (Mn 70,000–90000) and trifluoroethanol (TFE) were purchased from Sigma-Aldrich (St Louis, MO, USA) and gelatin (GE) was purchased from Shanghai Aladdin Biochemical Technology Co., LTD. (Shanghai, China). Carboxyl multiwalled carbon nanotubes (MWCNTsCOOH) were prepared by XFNANO (Neijing, China). PCL (0.7 g) and gelatin (0.3 g) were dissolved in 8 mL TFE, and MWCNT-COOH (0.03 g) was ultrasonically dispersed in 2 mL TFE. The liquids was mixed evenly and added to a 10 mL injection pump with a 20-gauge needle. Electrospinning parameters were set to: voltage 15 kV; flow rate 1 mL/h; roller speed 1000 rpm; working distance 15 cm. After electrospinning, PCL/GE/CNT fiber scaffold with thickness of 0.2 mm was obtained ed and vacuum dried at room temperature overnight.

2.2. The characterization of fiber scaffold

The surface morphologies of PCL/GE and PCL/GE/CNT scaffolds were observed by scanning electron microscopy (SEM) (JSM-7900F, JEOL, Tokyo, Japan). Fiber diameter distributions of the scaffolds were analyzed using Image-Pro Plus 6.0 software (Media Cybernetics, Rockville, MD, USA), and the water contact angles were measured by the water contact angle tester (OCA20, DataPhysitics, Filderstadt). The conductivity of the scaffolds was measured using a four-point probe system (RTS-9,4 PROBES TECH, Guangzhou, China). The elastic modulus and elongation at break of manufactured PCL/GE and PCL/GE/CNT scaffolds were measured using a universal testing machine (Model 5848,Instron, Norwood, 134 MA, USA).

2.3. The proliferation, migration and morphology of L929 cells and HUVEC cells

L929 cells and HUVEC cells were inoculated on PCL/GE group, PCL/GE/CNT group and PCL/GE/CNT-ES group at a density of 5×10^4/cm. The PCL/GE/CNT-ES group was stimulated with an electrode of 150 mV/mm and 0.1 Hz for 10 min every day. After 1, 3 and 5 days, the samples were washed with PBS and then incubated in 10 % CCK-8 solution. After incubation for 2 h, the absorbance of the solution at 450 nm was measured using a microplate reader (SpectraMaxM2, Molecular Devices, Sunnyvale, CA, USA). After 3 days of culture, the morphology of L929 cells and HUVEC cells grown on the scaffold was observed by SEM (JSM-7900F, JEOL) and confocal laser scanning microscope (CLSM, TCS-SP8, Leica). Additionally, after 3 days of culture, the samples were washed with PBS and then soaked overnight in 2.5 % glutaraldehyde (Sigma-Aldrich) solution at 4 °C. Next, the sample was dehydrated with graded ethanol, critically dried and coated with gold sputtering. Then, the morphology of L929 cells and HUVEC cells grown on the scaffold was observed by SEM (JSM-7900F, JEOL). Furthermore, the cell morphology was observed by CLSM. L929 cells was observed by staining with ghost pen cyclic peptide-alexa fluorescein 594/488 (Abcam). HUVEC cells were infiltrated with 0.1 % Triton X-100 for 5

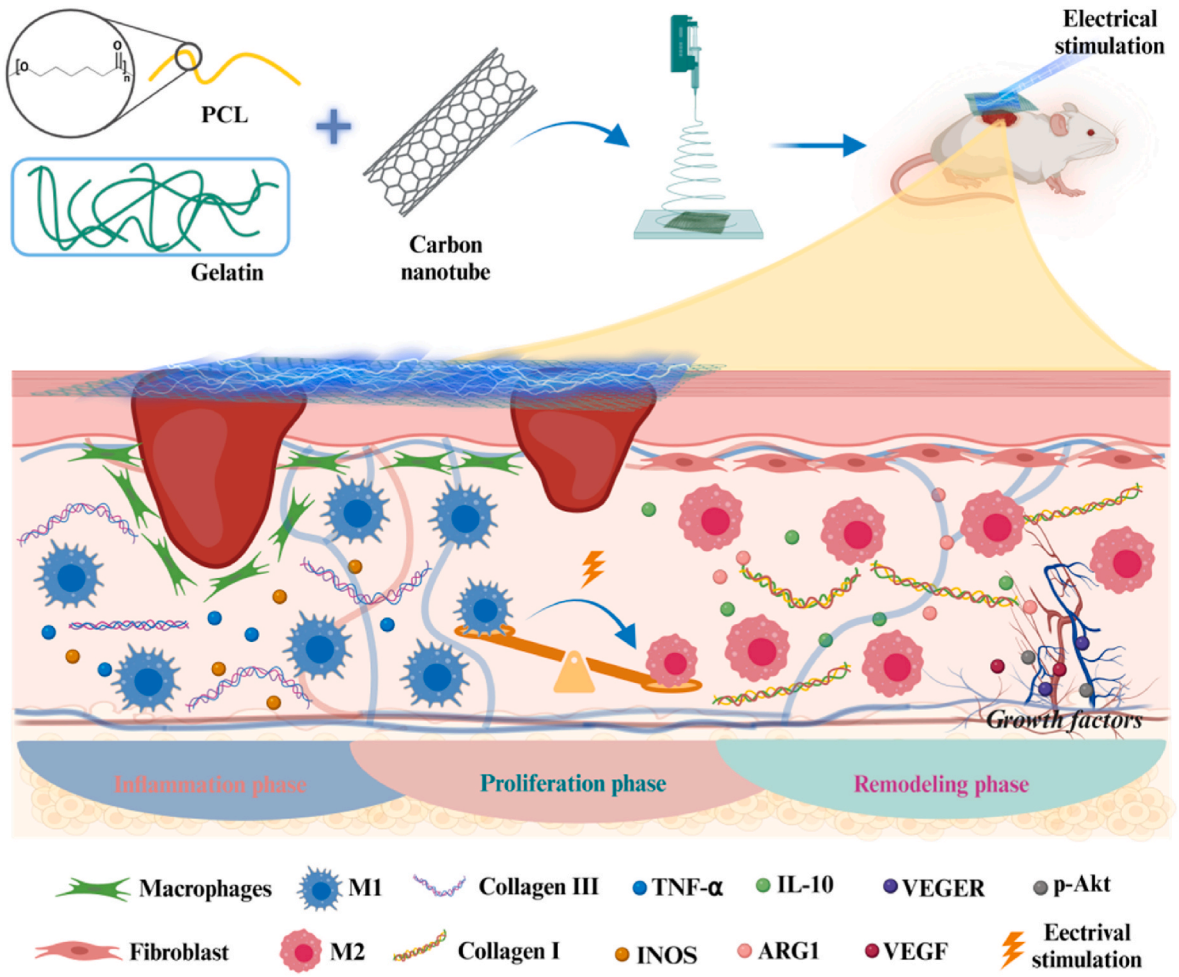

Scheme 1. PCL/GE/CNT electroactive scaffold derived from carbon nanotubes were constructed by electrospinning technology and combined with ES to promote skin repair. The scaffold, combined with local ES, participates in wound healing by regulating the behavior of macrophages, fibroblasts and endothelial cells. It can further accelerate wound healing process by achieving early remodeling of inflammatory microenvironment and promoting re-epithelialization, vascular regeneration and collagen deposition.

min and sealed with 2 % bovine serum protein at room temperature for 30 min. Next, CD31 (1:100, Abcam) was added and incubated at 4 °C overnight, then Alexa Fluor 488 Goat Anti-Rabbit IgG H&L (1:200, Abcam, USA) was incubated at room temperature for 1 h. 4′,6-diamidino-2-phenylindole (DAPI) were used to labeled nucleus.

L929 cells and HUVEC cells were inoculated on PCL/GE group, PCL/GE/CNT group and PCL/GE/CNT-ES group at a cell density of 5×10^5/well to form fusion monolayers. Then, use the tip of the sterilized pipette to gently scraped onto the fused cell layer. The PCL/GE/CNT-ES group was stimulated with an electrode of 150 mV/mm and 0.1Hz for 10 min every day. Cell migration was observed by microscope and the mobility was calculated. at 24 h and 48.

2.4. Macrophage phenotype modulation experiment

1×10^5 RAW 264.7 macrophages were inoculated on each group and incubated at 37 °C overnight for cell attachment. Subsequently, RAW 264.7 macrophages in each group were treated with LPS (100 ng/mL) and interferon (20 ng/mL) for 24 h to initiate M1 polarization. Control group of cells was inoculated on a petri dish. The PCL/GE/CNT-ES group was stimulated with an electrode of 150 mV/mm and 0.1Hz for 10 min every day. The cells were treated with 4 % paraformaldehyde fixation, 0.5 % Triton X-100 penetration, and 1 % bovine serum albumin blockade. Stain with TRITC-phalloidin/DAPI and observe by CLSM.

2.5. PCR real-time quantitative polymerase chain reaction

After 3 days of culture, total RNA of L929, HUVEC and RAW264.7 cells grown on the scaffolds was extracted using RNA purification kit (ES Science, Shanghai, China) and was reverse-transcribed using a reverse transcription kit (ABM, Vancouver, Canada). The quantitative real-time PCR was then performed using SYBR Green Realtime PCR Master Mix (TOYOBO, Osaka, Japan) on the CFX96TM real-time PCR system (Bio-Rad, Hercules, CA, USA). The expression of related genes was calculated by $2^{-\Delta\Delta Ct}$ method, and normalized against housekeeper gene GADPH. The list of primers for Col I, Col III, VEGF, eNOS, p-Akt, TNF-α, iNOS, IL-10 and Arg1 was shown in supplement material Table S1.

Perform differential expression gene (DEG) analysis using DESeq2, and determine significant differentially expressed genes based on $|\log2(\text{FoldChange})| > 0.5$ and $p < 0.05$. Perform GO functional enrichment analysis and KEGG pathway enrichment analysis on differential gene sets using clusterProfiler software.

2.6. The biosafety assessment in vivo

To evaluate the biocompatibility and degradability of scaffold in vivo, we anesthetized SD rats with pentobarbital sodium. After the incision on the back skin, a 20 mg sample was implanted. In the blank control group, only skin incision and suture were performed without embedding any material. The positive control group was filter paper.

The skin reaction of each group was observed at 0,3,7,14 days. After 14 days, the rats in each group were euthanized, and the whole skin tissue of each group was stained with hematoxylin-eosin (HE). Then the skin pathological changes (especially foreign body reaction and inflammatory reaction) were observed, and the degradation performance of the material was evaluated. In addition, the HE staining of heart, lung, liver, spleen and kidney in blank group and PCL/GE/CNT group were observed.

2.7. The full skin defect model of SD rats

All experimental procedures in this study were carried out in accordance with ethical guidelines and approved by the Animal Ethics Committee of Peking University People's Hospital (approval number: 2021PHE067). Each experimental animal was randomly divided into 4 groups with 10 animals in each group: control group (no treatment), PCL/GE group, PCL/GE/CNT group, and PCL/GE/CNT-ES group.

After anesthesia, the back hair of the rats was removed, and the skin defect wound with a diameter of 1 cm was made in the middle of the dorsal side with a skin punch. Skin defects were covered with the corresponding composite scaffold for each group except control group. In order to record the healing process of the wound, the wound was photographed at 0, 3, 7 and 14 days after treatment. The calculation formula of wound healing rate is: wound healing rate $=(A_0 - A)/(A) \times 100\ \%$, where A_0 is the initial wound area and A is the current wound area.

2.8. Histological and immunohistochemical analyses

The rats were killed at a specific time point, and specimens were collected and fixed in 4 % PFA for 24 h, and paraffin embedding was performed for histological and immunohistochemical evaluation. HE staining and Masson staining were used to evaluate the pathological status and healing of the wound. Col I, Col III, and CD31 immunostaining were used to evaluate collagen and neovascularization during healing. The levels of TNF-α and IL-6, and the inflammatory response of the grafts was detected by immunofluorescence staining. All images were taken using fluorescence microscopy.

2.9. Statistic analysis

Quantitative results were obtained for at least 5 samples in each group, and the experiment was repeated for at least 3 times. The resulting data was preprocessed using Excel (Microsoft, USA). All quantitative data are expressed as mean ± standard deviation. Statistical software SPSS, Version 19.0 (SPSS Inc., Chicago, IL, USA), univariate or two-factor analysis of variance (ANOVA) and Tukey postmortem test were used to analyze the statistical difference between the experimental results. $p < 0.05$ was considered statistically significant. The statistical tests conducted in this study are also represented by legends: *$p < 0.05$, **$p < 0.01$.

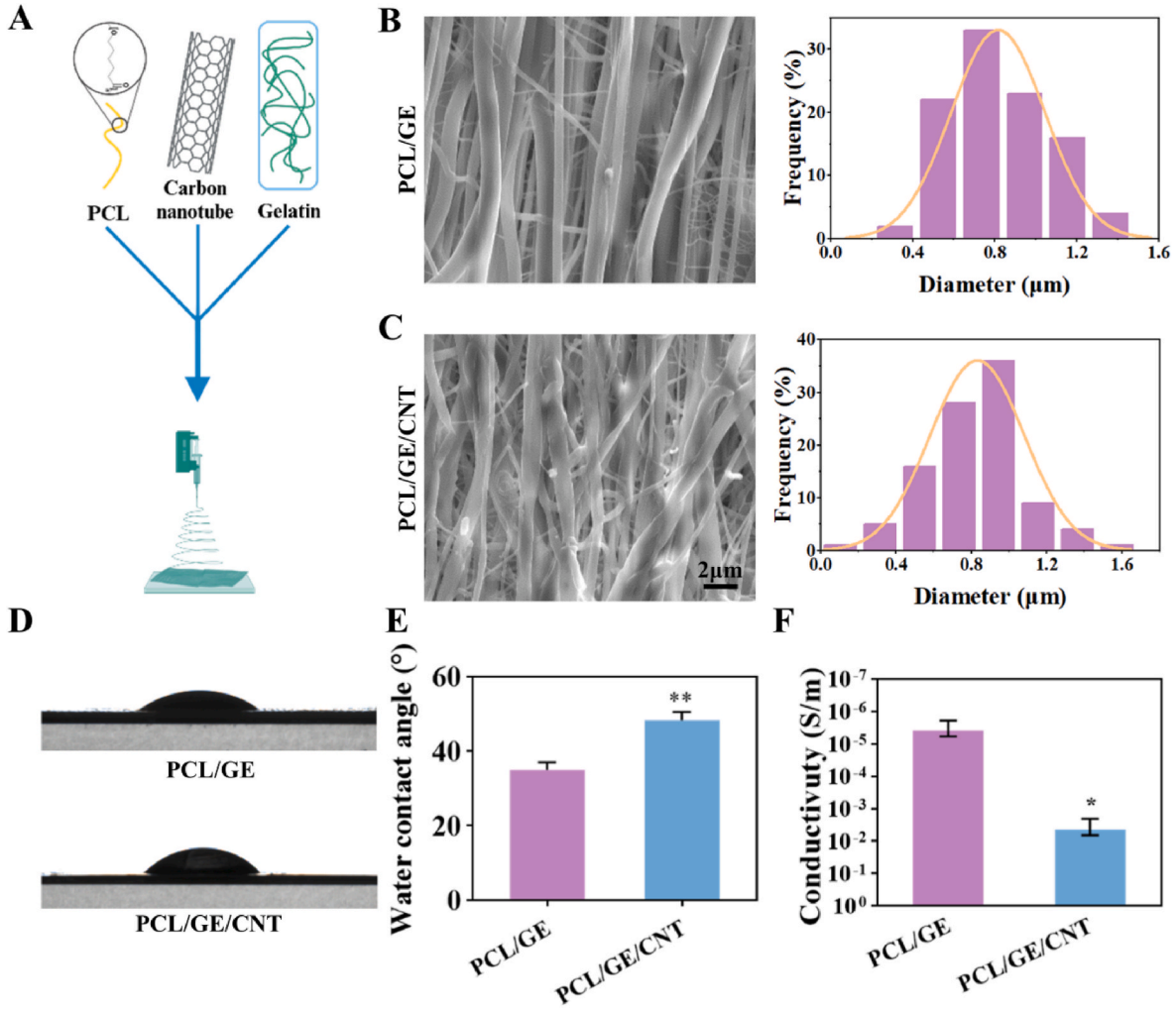

Fig. 1. (A) Schematic diagram of the preparation process of PCL/GE/CNT scaffold. SEM images and fiber diameter distribution of (B) PCL/GE and (C) PCL/GE/CNT. (D, E) Water contact angle and (F) conductivity of PCL/GE and PCL/GE/CNT.

3. Result and discussion

3.1. Characterization of scaffolds

In the process of application, the surface morphology of wound repair materials directly or indirectly affects their biological functions. In this study, surface structures of different materials were obtained by scanning electron microscopy (SEM). According to Fig. 1B and C, PCL/GE and PCL/GE/CNT fiber scaffold both have smooth surfaces, and it also shows the directional arrangement of PCL/GE/CNT scaffold.

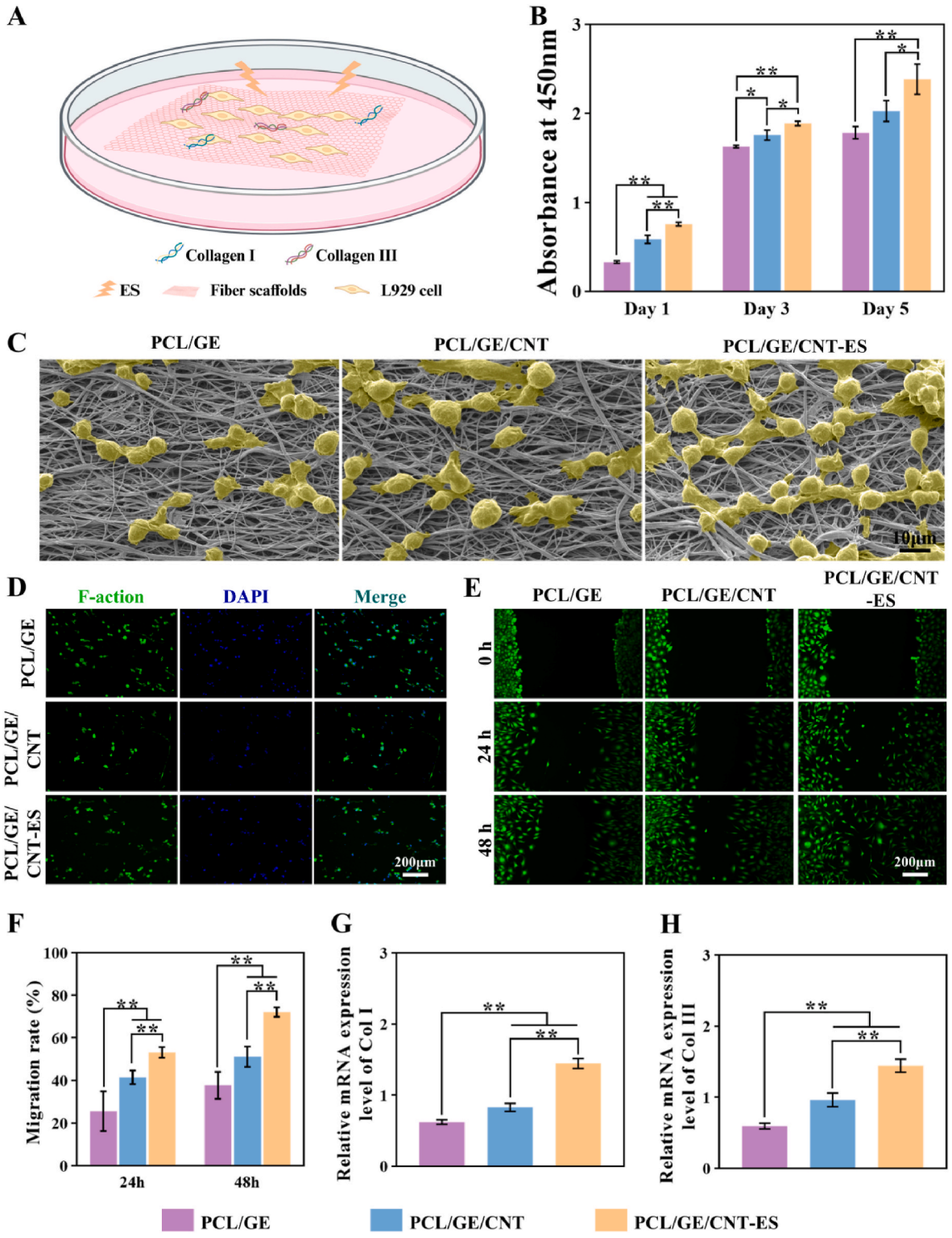

Fig. 2. (A) Schematic diagram of PCL/GE/CNT scaffold promoting fibroblasts releasing collagen-related substances. (B) Cell viability of L929 cells in PCL/GE, PCL/GE/CNT and PCL/GE/CNT-ES group (n = 4, *p < 0.05, **p < 0.01, ***p < 0.001). (C) SEM images of L929 cells on the surface of fiber scaffold. (D) CLSM of L929 cells with F-actin/DAPI staining. (E) Cell migration pictures and (F) migration rate of scratch assay. Expression levels of (G) Col I and (H) Col III in L929 cells for culturing 3 days.

Additionally, the average diameter of PCL/GE/CNT (0.83 ± 0.25 μm) was similar to that of PCL/GE (0.82 ± 0.23 μm) (Fig. 1B and C), indicating that the addition of a small amount of CNT did not significantly change the diameter of the nanofibers.

During wound healing, the management of wound exudates is essential to promote chronic wound healing. Wound exudates can promote the migration and proliferation of fibroblasts and endothelial cells. However, excess exudate from the wound will cause persistent inflammation [20]. Fibrous membranes with hydrophilic properties can promote the absorption of fluid at the wound site and facilitate the formation of blood clots. However, when the hydrophilicity of the materials is too strong, the wound dressing will adhere to the surface of the new tissue, increasing the pain and difficulty of dressing change [19]. In addition, in the process of wound healing, the characteristics of wound dressing surface have a great influence on cell adhesion, proliferation and biosynthesis. Previous studies have shown that cells tend to adhere and proliferate more easily in moderately hydrophilic surface, which is defined as a water contact angle between 40 and 70° [21]. In this study, we evaluated the hydrophilicity of different materials by measuring the water contact angle. The surface of a material is considered hydrophilic when the water contact angle is between 10° and 90° [22]. As shown in Fig. 1D, the results show that both PCL/GE and PCL/GE/CNT have hydrophilic surfaces. The water contact angle of PCL/GE and PCL/GE/CNT are 35.04 ± 1.99° and 48.22 ± 2.37°, respectively. Our previous study showed that the water contact angle of PCL was 111.47 ± 1.09° [23], and after the addition of GE, the water contact angle of the material decreased significantly, indicating that the addition of GE can improve the hydrophilicity of PCL and make the material more conducive to cell adhesion, migration and proliferation. In addition, compared with PCL/GE, the water contact angle of PCL/GE/CNT is slightly increased, proving that the introduction of CNT can appropriately reduce the hydrophilicity of the material and avoid the negative impact caused by too strong hydrophilicity of the material. This may create a more suitable environment for skin wound healing, and also provide better conditions for the clinical application of PCL/GE/CNT.

CNT was selected as a conductive component to give PCL/GE conductive property, because of its good electrical conductivity, biocompatibility and chemical stability [14]. The conductivity of these scaffolds was shown in Fig. 1F. The conductivity of PCL/GE was low ($3.81 \times 10^{-6} \pm 1.92 \times 10^{-6}$ S/m). In contrast, the conductivity of PCL/GE/CNT increased ($4.31 \times 10^{-3} \pm 2.28 \times 10^{-3}$ S/m) and was consistent with that of normal skin (1×10^{-4} to 0.26 S/m) [24], which thanks to the addition of CNT. Dressings with conductive properties can enhance endogenous currents in the skin, improve the migration of neutrophils, macrophages, and keratinocytes to the wound site, regulate the inflammatory response and promote angiogenesis [25]. Therefore, these conductive wound dressings, which display electrical conductivity similar to that of skin, would greatly benefit wound healing.

3.2. Effect on the behavior of L929 cells

In this study, we used the CCK-8 assay to detect the proliferation of L929 cells under different scaffold materials and conditions. Fig. 2B showed that both CNT and ES showed positive stimulation on the proliferation of L929 cells after culturing several days, and PCL/GE/CNT-ES group showed higher stimulation on the cell proliferation than PCL/GE/CNT. Fig. 2C and D showed the diffuse morphology of L929 cells growing on the surface of the three scaffolds after 3 days. The cells on PCL/GE, PCL/GE/CNT and PCL/GE/CNT-ES were well dispersed and evenly distributed. This showed that L929 cells attached well to the surface of the scaffold, and the three scaffold materials did not affect cell viability and have no cytotoxicity. In addition, it is worth noting that although PCL/GE fiber scaffold cells are well grown, the number of cells is small. Compared with PCL/GE group, PCL/GE/CNT and PCL/GE/CNT-ES had more adherent cells and larger adherent area. These results further confirmed the positive role of CNT and ES in promoting cell attachment and proliferation.

Fibroblast migration plays an important role in wound re-epithelialization and closure. The ability of ES and different scaffolds to promote cell migration was investigated by cell scratch tests (Fig. 2E). After 48 h of treatment, the results of the closure area showed significant differences between the PCL/GE group and the PCL/GE/CNT and PCL/GE/CNT-ES group (Fig. 2F). PCL/GE/CNT and PCL/GE/CNT-ES group were able to induce L929 cells to migrate at a significantly faster rate, while cells in the PCL/GE group showed a slower rate of migration. These results indicate that PCL/GE/CNT composite fiber scaffolds combined with ES can significantly promote cell migration.

Fibroblasts are the main cells that release type I collagen (Col I) and type III collagen (Col III) during wound healing [26]. Col I is a major protein in the extracellular matrix (ECM), and its gene expression is present at every stage of wound repair process [27]. Col I can directly promote the adhesion and migration of a variety of cells, including keratinocytes and fibroblasts [28]. For Col I gene expression (Fig. 2G), PCL/GE/CNT-ES group showed higher mRNA expression levels than PCL/GE and PCL/GE/CNT. During proliferation stage of wound healing, the connective tissue and granulation tissue composed of Col III can be used as scaffolds to form new ECM [29]. For the gene expression of Col III (Fig. 2H), the expression of gene in PCL/GE/CNT-ES group was also significantly higher than that in other groups. The reason may be that ES promotes the proliferation and migration of fibroblasts and accelerates collagen deposition and re-epithelialization process [24]. At the same time, ES can promote the attachment of L929 on the surface of PCL/GE/CNT, while PCL/GE/CNT-ES can maintain the biological activity of cells and provide recognition sites for their growth, so as to more effectively promote the expression of Col I and Col III. These results indicate that PCL/GE/CNT-ES is most effective in promoting the expression and translation of tissue repair related molecules, which further indicates that PCL/GE/CNT-ES has a more positive effect than PCL/GE/CNT on improving the tissue repair ability.

3.3. Effect on the behavior of HUVEC cells

HUVEC cells were used to investigate the effect of the scaffold on angiogenesis (Fig. 3A). The effect of the scaffolds and ES on the proliferation of HUVEC cells was tested by CCK-8 cell count analysis. The results showed that the proliferation of HUVEC cells was significantly enhanced with PCL/GE/CNT-ES group (Fig. 3B). Fig. 3C and D showed that the number of cells on PCL/GE/CNT-ES group was the highest in the three groups, indicating the strongest ability to promote the proliferation of HUVEC cells. In addition, the results showed that most of the cells maintained normal morphology and showed good proliferative activity after culture, indicating that all three fiber scaffolds had good biocompatibility.

The wound healing process involves the coordination and integration of multiple biological processes such as cell migration and proliferation, collagen deposition, and angiogenesis [30]. Among them, angiogenesis involves several biological processes such as endothelial cell proliferation, migration, and tube formation [31]. The newly formed blood vessels can deliver nutrients and oxygen to the wound, thus accelerating wound healing [32]. This study evaluated the role of fiber scaffolds in promoting angiogenesis by HUVEC cell scratch test. The experimental results showed that HUVEC cell mobility in PCL/GE/CNT-ES group was superior to that in PCL/GE and PCL/GE/CNT groups after co-incubation with various samples for 48 h (Fig. 3E and F). These results indicate that PCL/GE/CNT combined with ES presents better performance in promoting cell migration and angiogenesis.

VEGF is considered to be an important regulator of angiogenesis during tissue repair. It has been shown to induce angiogenesis and granulation tissue formation, thereby promoting wound repair [33]. When VEGF binds to the corresponding receptor, it activates several downstream signaling molecules, including p-Akt, which has a

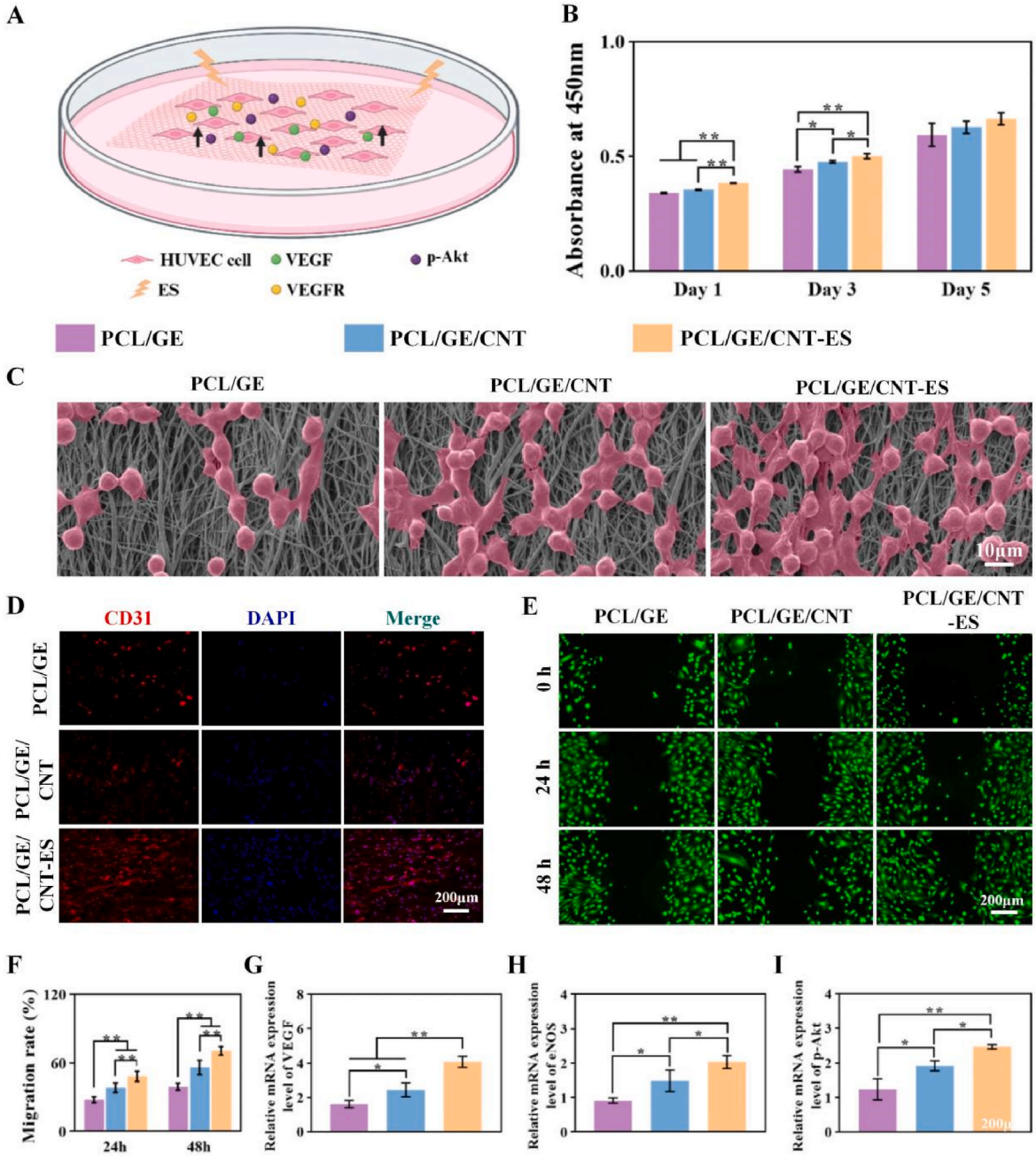

Fig. 3. (A) Schematic diagram of the coculture. (B) Cell viability of HUVEC cells in PCL/GE, PCL/GE/CNT, and PCL/GE/CNT-ES. (C) SEM images of HUVEC cells on the surface of fiber membrane. (D) CLSM of HUVEC cells with CD31/DAPI staining. (E) Cell migration picture and (F) migration rate in scratch assay of HUVEC cells. Related gene expression levels of (G) VEGF, (H) eNOS, and (I) p-Akt in HUVEC cells.

long-term impact on the function of vascular endothelial cells [32,34]. To further evaluate the angiogenesis performance and mechanism of the fiber scaffold, mRNA levels of VEGF, eNOS, and p-Akt were measured (Fig. 3G–I). The results showed that the PCL/GE/CNT-ES group had higher levels of VEGF, eNOS and p-Akt gene expression than the other two groups. These results suggest that PCL/GE/CNT-ES may promote angiogenesis by increasing the expression of VEFG.

3.4. Regulation immune response in vitro

Inflammation is initial response to typical wound repair. Macrophages are one of the important early inflammatory indicators and play a key role in inflammation [35]. Normally, in the early stages of wound healing, macrophages appear to be pro-inflammatory (M1), which mediate the defense response and remove pathogens and cell debris from the wound site. It is subsequently converted to the anti-inflammatory type (M2), which suppresses inflammation and promotes tissue remodeling and repair [36]. However, after tissue injury, there is often excessive release of inflammatory factors (inflammatory storm), which aggravates the tissue injury and hinders the tissue repair process. Previous studies have shown that ES can effectively regulate the immune microenvironment at the wound site by regulating the polarization of macrophages and promoting the transformation of macrophages from M1 type to M2 type [37]. Recent studies have shown that ES can also significantly improve macrophage phagocytosis and selectively regulate cytokine production [38]. In order to investigate the effect of PCL/GE/CNT-ES on the immune microenvironment at the wound site, macrophage phenotype regulation experiment and

immunofluorescence staining assay was conducted to observe the effect of scaffold on the phenotype of macrophages. As shown in Fig. 4B–D, M1 was marked by iNOS/DAPI and M2 was marked by Arg1/DAPI. It showed that RAW 264.7 cells growth on PCL/GE/CNT-ES had more M2 type and fewer M1 type than the other groups (Fig. 4C and D). Several cytokines play an important role in the regulation of macrophages phenotypic transformation. The expression levels of the pro-inflammatory factor TNF-α and the anti-inflammatory factor IL-10, as well as the M1 macrophage marker iNOS and M2 macrophage marker Arg1 were analyzed by PCR. Among them, Arg1 can promote collagen synthesis and epithelial cell proliferation, and IL-10 can inhibit pro-inflammatory cell activation, migration and adhesion [39]. The results showed that PCL/GE/CNT-ES could reduce inflammation by down-regulating TNF-α and iNOS, and up-regulating IL-10 and Arg1 (Fig. 4E–H).

3.5. Evaluation of biosafety in vivo

In order to evaluate the biocompatibility of PCL/GE/CNT scaffolds in vivo, filter paper (control group), PCL/GE scaffolds, and PCL/GE/CNT scaffolds were implanted into the subcutaneous tissues of the back of rats, and wound conditions were observed on day 3, day 7 and day 14 (Fig. 5A and B). On the 7th day, the wounds of the control group showed obvious redness and swelling. After 14 days, all wounds had fully recovered. In addition, HE results showed that the control group had more severe foreign body granulomas and inflammatory reactions, while the other groups remained normal, indicating that the PCL/GE/CNT scaffold showed good biocompatibility in vivo.

In order to further investigate the biotoxic effects of scaffolds on other organs, including spleen, kidney, heart, liver and lung, HE staining of those organs in the blank group and PCL/GE/CNT group on day 14 was compared. HE staining results (Fig. 5C) showed that no obvious damage was found in the organs of rats with PCL/GE/CNT implanted, indicating that PCL/GE/CNT and its metabolites had no obvious adverse effects on the circulatory system, respiratory system, digestive system and metabolic system.

3.6. Evaluation of promoting wound healing

After establishing rats full-layer skin defect model, the wound was covered with PCL/GE and PCL/GE/CNT, and the wound healing status was observed and recorded on day 3, day 7 and day 14 after surgery. On day 3, the PCL/GE, PCL/GE/CNT, and PCL/GE/CNT-ES groups developed scabs on their wounds. This wound state corresponds to the phase of proliferative healing, with the characteristics of wound contraction, collagen deposition, and new tissue formation. But the control group did

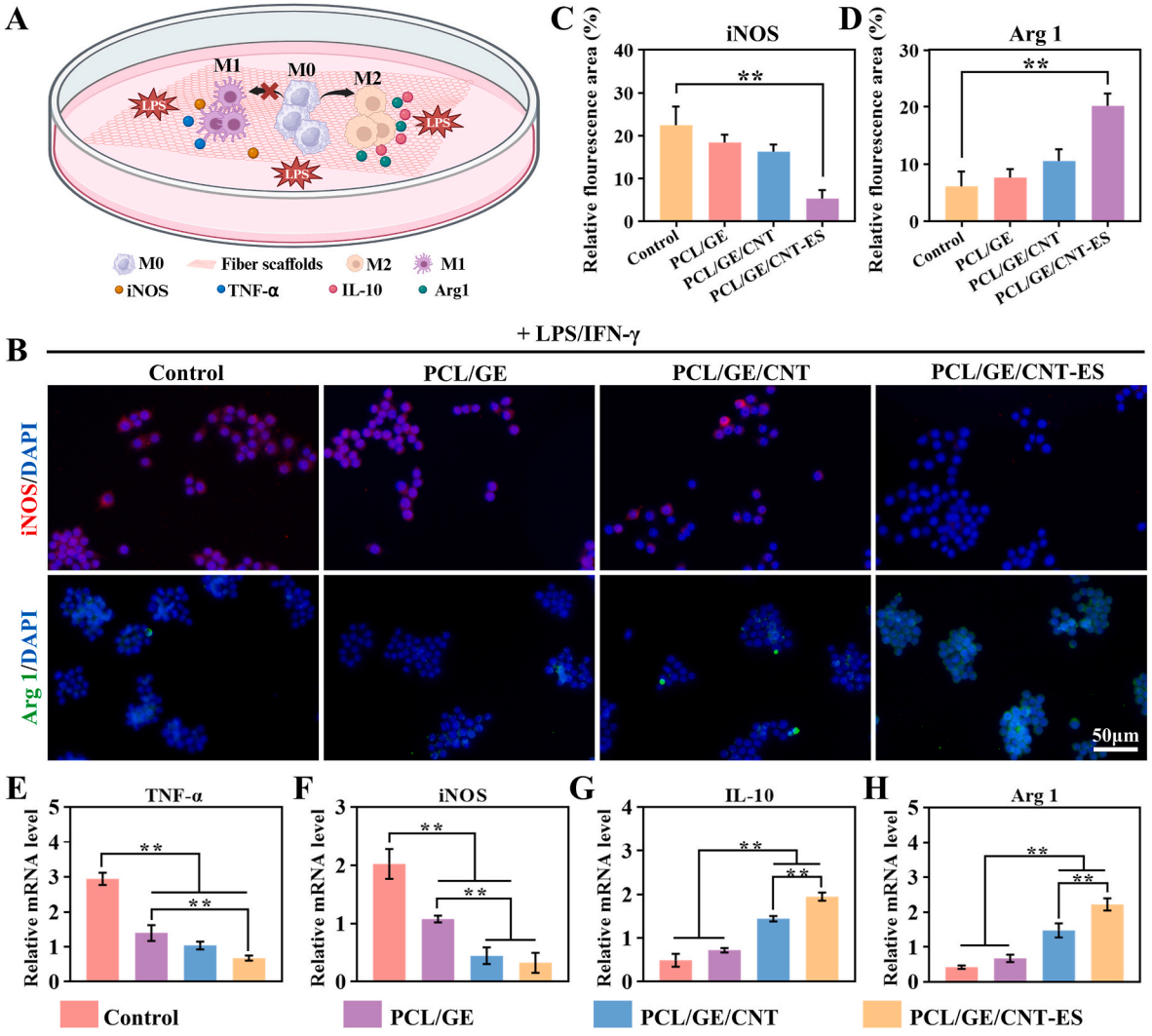

Fig. 4. (A) Schematic diagram of scaffold regulating release of relevant factors. (B) Immunofluorescence staining of RAW 264.7 after co-treatment of LPS/IFN-γ and scaffold (iNOS/DAPI: M1 macrophage; Arg1/DAPI: M2 macrophage). Relative flourescence area of (C) iNOS and (D) Arg1. Relative mRNA expression levels of (E) TNF-α, (F) iNOS, (G) IL-10 and (H) ARG1 in RAW264.7 cells.

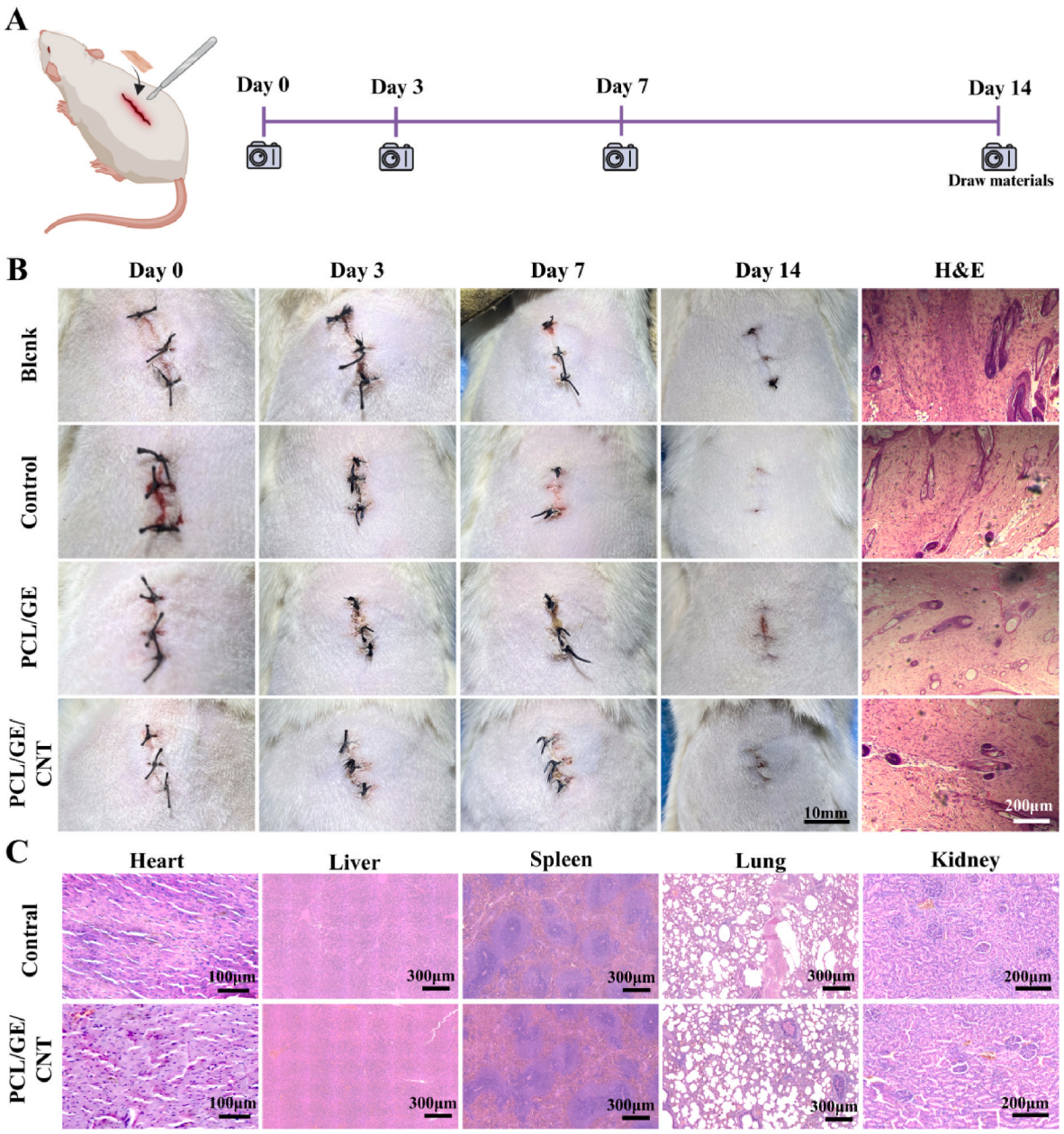

Fig. 5. (A) Schematic diagram of subcutaneous embedding in rats. (B) Wound healing photos at days 0, 3, 7 and 14 and skin HE staining images at days 14. (C) HE staining images of heart, liver, spleen, lung and kidney in blank group and PCL/GE/CNT group after 14 days of embedding.

not. At the end of the proliferative phase, collagen fibers cross-link and replace the scab, resulting in complete coverage of the wound and causing the scab to fall off. The results showed that the scab fragments in PCL/GE/CNT and PCL/GE/CNT-ES groups were all shed by day 7, but not in the control group and PCL/GE group. In addition, wound size decreased over time in all groups. Compared with day 0, wound healing rates in the control group, PCL/GE and PCL/GE/CNT groups reached 66.75 %, 81.70 % and 83.88 % on day 14 (Fig. 6D). The wound healing rate in PCL/GE/CNT-ES (91.86 %) group was significantly higher than that in the other three groups. It was shown that PCL/GE/CNT-ES was better at promoting wound healing than PCL/GE and PCL/GE/CNT (Fig. 6B and C).

The role of ES in wound healing is not only limited to physical stimulation, but also includes regulating the immune response by regulating the expression of cytokines. Both TNF-α and IL-6 are important pro-inflammatory cytokines, and their high expression is often associated with acute and chronic inflammatory responses. To further verify the immunomodulatory mechanism of ES in promoting wound healing, we analyzed the expression of TNF-α and IL-6 in newborn tissues by immunofluorescence staining (Fig. 7E and F). These cytokines play an important role in inflammatory response and immune regulation, so their expression changes can reflect the effect of electrical stimulation on immune response. By analyzing the percentage of TNF-α and IL-6 positive area, we found that the percentage of TNF-α and IL-6 positive area in PCL/GE/CNT-ES group was always significantly lower than that in control group, PCL/GE group and PCL/GE/CNT group on day 7 and day 14. This suggests that ES, when combined with PCL/GE/CNT scaffold, can more effectively reduce the inflammatory response, thereby promoting wound healing.

3.7. Histological analysis

As shown in Fig. 7A, granulation tissue was thicker and scar width was narrower in PCL/GE/CNT-ES group compared with other groups. As

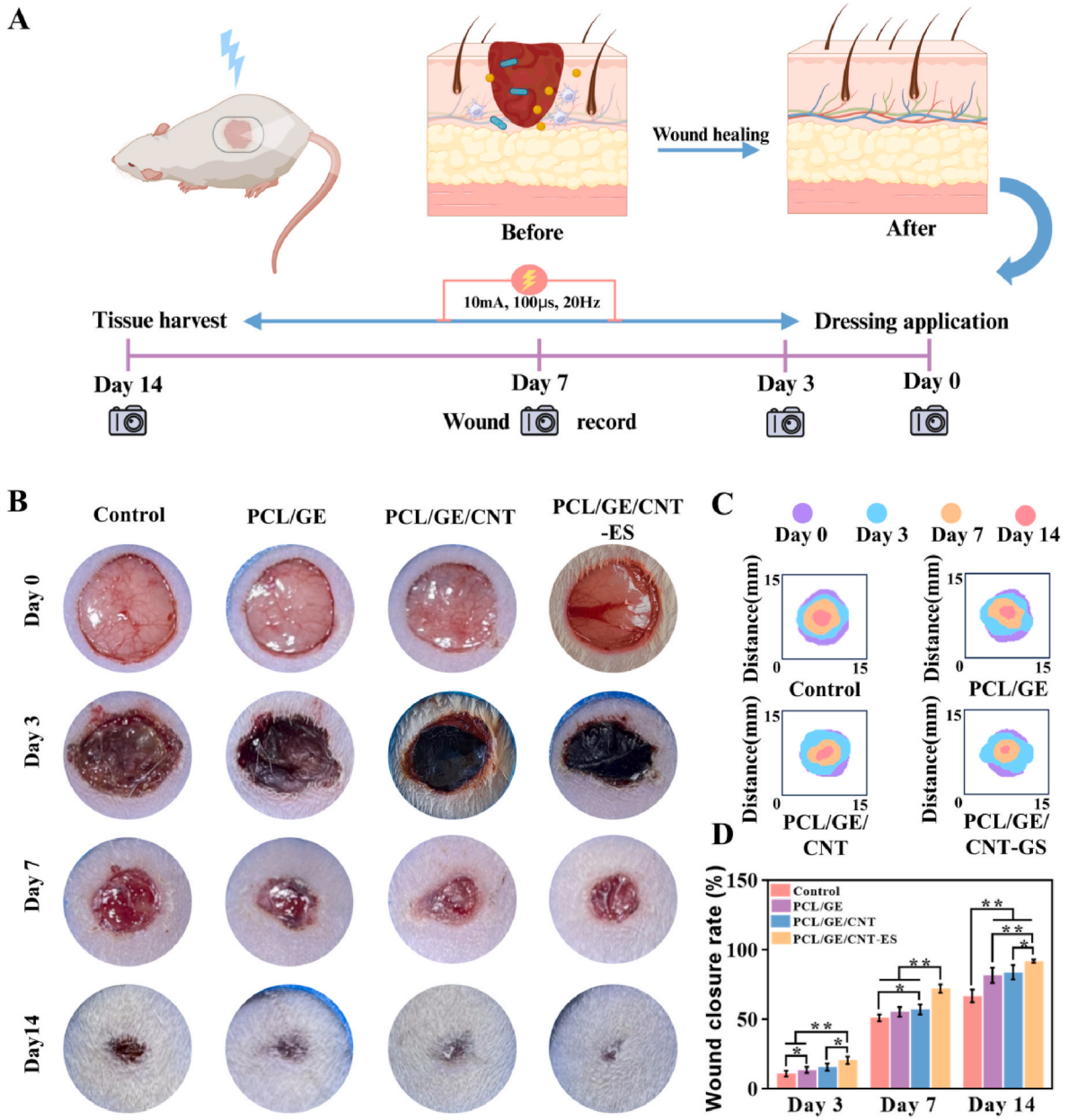

Fig. 6. (A) Schematic diagram of PCL/GE/CNT scaffold combined with electrical stimulation to promote wound healing. (B) Photographs of the healing process of skin wounds at 0, 3, 7, 14 days and (C) quantified maps of the healing process. (D) Healing process histogram at 3, 7, 14 days.

can be seen from Fig. 7B, the scar width in PCL/GE/CNT-ES group (813.18 ± 7.62 μm) was significantly lower than that in control group (2054.26 ± 145.03 μm), PCL/GE/CNT group (1453.49 ± 47.07 μm) and PCL/GE group (1368.22 ± 23.89 μm). In addition, as shown in Fig. 7C, on the 14th day, the granulation tissue thickness of PCL/GE/CNT-ES group (1476.74 ± 18.99 μm) was greater than that of the control group (1104.65 ± 18.99 μm) and PCL/GE/CNT group (1279.07 ± 47.47 μm). PCL/GE group (1259.69 ± 19.76 μm). These data showed that the PCL/GE/CNT-ES group had a better ability to promote wound healing than the other groups. This is attributed to: PCL/GE/CNT provides a high-affinity platform to guide cell migration to locate at the wound site for the generation of new tissue. Additionally, under ES, PCL/GE/CNT can better enhance endogenous wound current, promotes blood circulation, reduce scar formation and alleviate pain at the same time [40].

3.8. Angiogenesis and collagen secretion in vivo

Angiogenesis is a key process in accelerating tissue healing [41]. Immunofluorescence of CD31 was further used to observe the formation of blood vessels at the wound site. As shown in Fig. 7D, PCL/GE/CNT-ES group had stronger fluorescence intensity compared with the other group. The results indicated that PCL/GE/CNT-ES group had higher vascular density, which was consistent with the in vitro experiment.

Masson staining was used to further evaluate the effect of the scaffold on promoting skin healing in vivo. As shown in Fig. 8A, the epidermis of the new granulation tissue was integrated and thickened in the PCL/GE/CNT-ES group. Furthermore, in the PCL/GE/CNT-ES group, not only new hair follicles were clearly produced in the wound center, but also proliferating fibroblasts and orderly and sufficient collagen deposition were detected under the epidermis, which was not seen in the control group. In addition, as can be seen from Fig. 8D, hair follicle density in PCL/GE, PCL/GE/CNT and PCL/GE/CNT-ES group increased

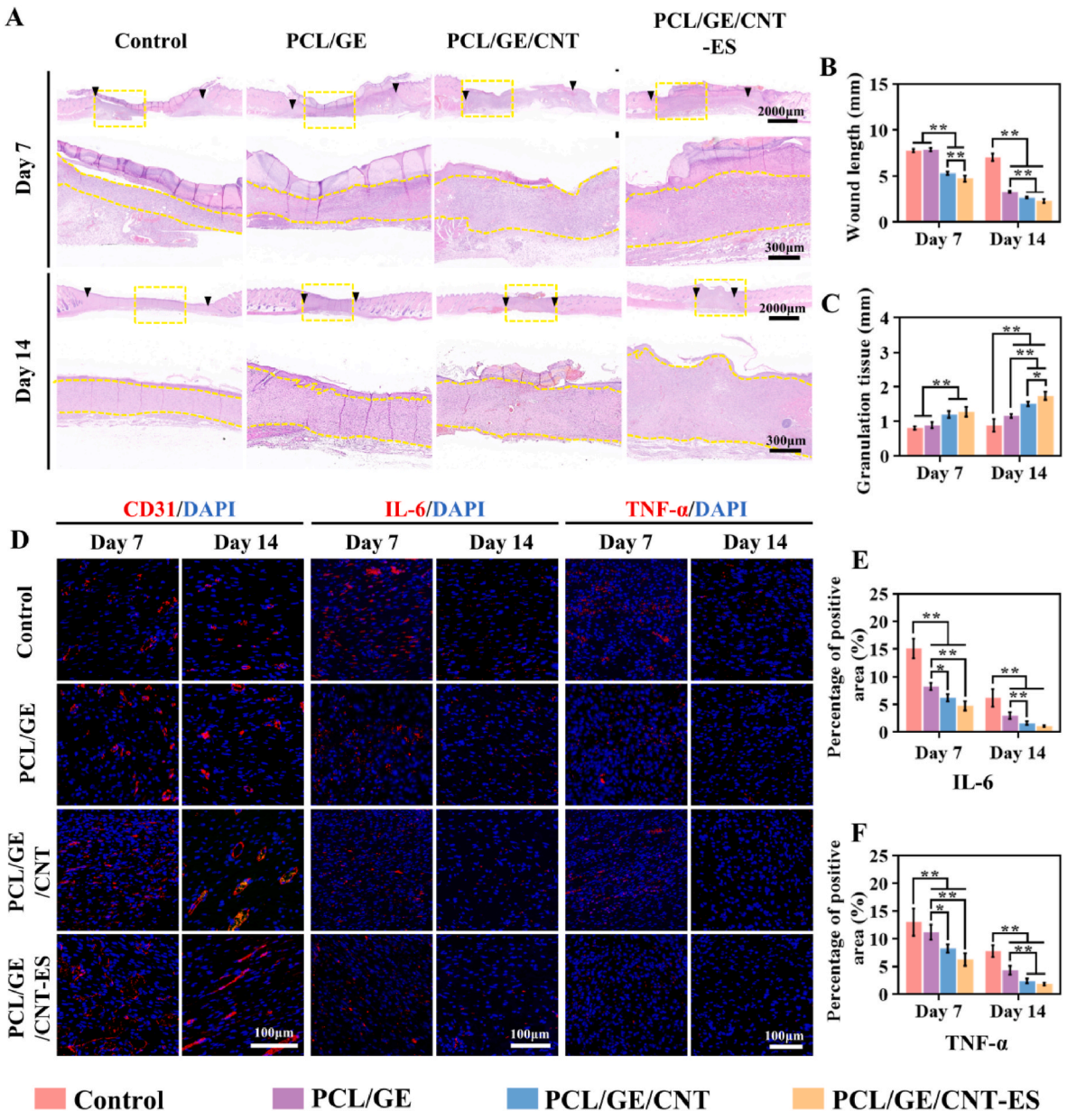

Fig. 7. (A) HE staining images of wounds in control group, PCL/GE, PCL/GE/CNT and PCL/GE/CNT-ES group at 7 and 14 days after treatment. The dashed lines represent the regenerated dermis and granulation tissue, and the arrows indicate the scar width. (B) Scar tissue width, (C) granulation tissue thickness, (D) CD31, TNF-α and IL-6 immunofluorescence staining images of the control group, PCL/GE, PCL/GE/CNT and PCL/GE/CNT-ES group at day 7 and 14 after treatment. The percentage of positive area for (E) IL-6 and (F) TNF-α.

significantly on day 7 and day 14 compared with control group, PCL/GE and PCL/GE/CNT-ES group.

Col I and III are the main ECM components in the dermis, and their formation plays an integral role in wound healing. Proper collagen deposition and remodeling can enhance the tensile strength of tissues and lead to better healing results. Therefore, immunostaining was used to investigate the content of Col I and Col III in wound tissue. At days 7 and 14, the newly formed collagen deposition in PCL/GE/CNT-ES group was significantly more than in other wounds (Fig. 8B and C). As shown in Fig. 8E and F, the deposition amounts of Col I and III showed a change pattern similar to that of Masson staining. Col I and III deposits increased in all wounds as healing time increased. These data indicate that PCL/GE/CNT-ES can accelerate collagen deposition at the wound site, and improve the healing quality of wound tissue.

3.9. Mechanism of PCL/GE/CNT combined electrical stimulation to promote wound healing

To further analyze the mechanism of action of electrical stimulation to promote repair, we performed transcriptome sequencing on the samples. Non-electrically stimulated wound tissue was the control group. After transcriptional sequencing and analysis of 3 samples of electrical stimulation and non-electrical stimulation, it was found that there were 944 differentially expressed genes (DEGs), including 205 up-regulated genes and 739 down-regulated genes (Fig. 9A). The DEGs were further clustered according to the high and low genes set (Fig. 9B). Gene ontology(GO)and Encyclopedia of Genes and Genomes (KEGG) analysis showed that electrical stimulation regulated immune responses, cytokine-cell interactions, extracellular matrix and cellular adhesion, which were involved in tissue repair process (Fig. 9C and D). In addition, GASE analysis further revealed that in addition to the extracellular

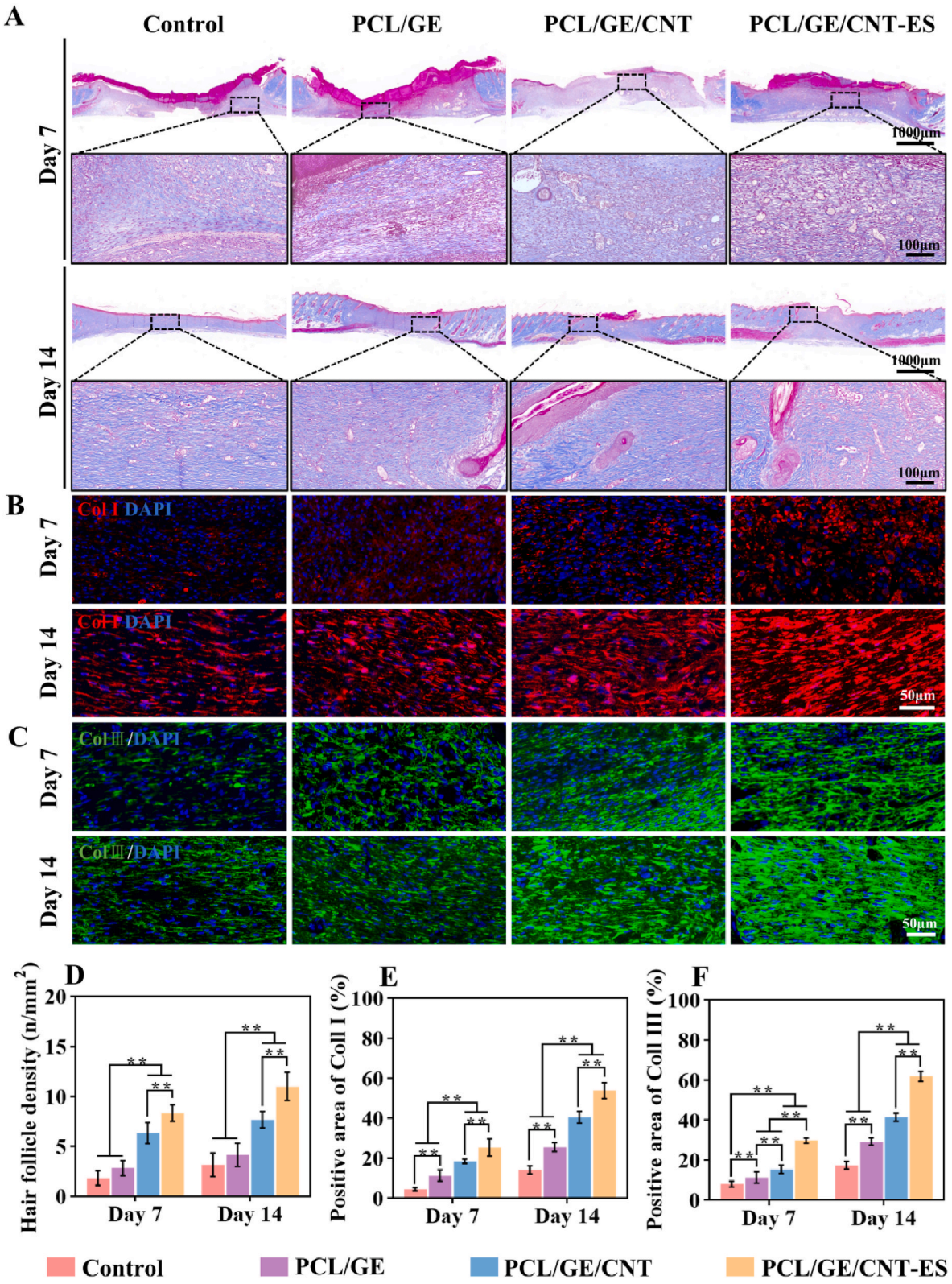

Fig. 8. (A) Masson-stained sections of wounds. Immunohistochemical staining of (B) Col I and (C) Col III at the wound site on day 7 and 14. (D) Hair follicle density of the wound site at day 7 and 14. (E) Col I and (F) Col III immunohistochemical staining positive area.

matrix, Metallopeptidase activity was also regulated (Fig. 9E and F). We noted that the wound healing and angiogenesis gene TGF-β1, the ECM proliferation gene Col 7A1, and the immune cell influx gene IL6 were differentially expressed in the electrical stimulation and control groups (Fig. S1). Those results further confirm that electrical stimulation could promote wound healing and repairment by immune modulation and extracellular matrix pathways.

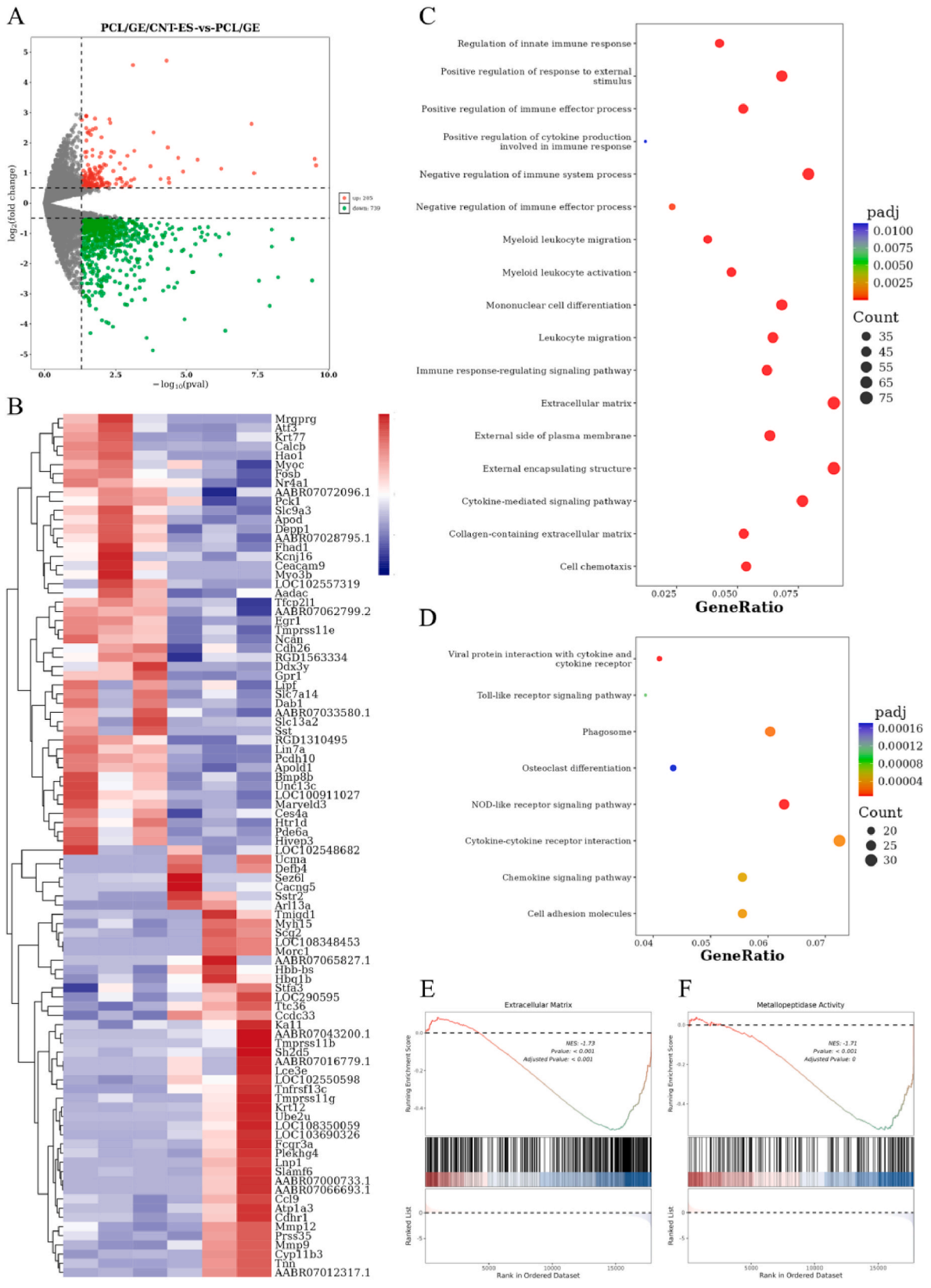

Fig. 9. (A) The volcano map shows upregulated and downregulated genes. (B) Heatmap of gene expression level. (C) Gene ontology (GO) and (D) Kyoto encyclopedia of genes and genomes (KEGG) pathway enrichment analysis. (E) Selected gene set enrichment analysis (GSEA) enrichment scoring curve.

4. Conclusion

In summary, we demonstrated that a directed nanofiber dressing based on carbon nanotubes and polycaprolactone/gelatin scaffold can accelerate the healing process of skin wounds under ES. PCL/GE/CNT scaffolds have multiple functions, including ideal mechanical properties, hydrophilicity, electroactivity, good biodegradability, and biosafety. In vitro and in vivo assays have shown that PCL/GE/CNT scaffolds can effectively promote the adhesion and proliferation of L929 cells and HUVEC cells, increase the expression levels of genes related to wound healing such as Col I/III and VEGF, and accelerate the wound healing process. Transcriptome sequencing and immunofluorescence analysis further revealed the molecular mechanism by which electrical stimulation promotes wound healing and repair by regulating immune responses and extracellular matrix pathways. Especially the significant decrease in the expression of TNF-α and IL-6 indicates that electrical stimulation effectively reduces inflammatory response. Overall, the PCL/GE/CNT stent combined with ES is not only easy to manufacture and apply, but also shows great potential in future clinical applications as wound dressings. This study provides important experimental basis and theoretical guidance for the development of skin tissue engineering.

CRediT authorship contribution statement

Weizhi Chen: Writing – original draft, Visualization, Methodology, Investigation, Formal analysis, Data curation, Conceptualization. **Yiliu Wei:** Writing – original draft, Visualization, Methodology, Investigation, Conceptualization. **Jing Chang:** Writing – review & editing, Writing – original draft, Visualization, Methodology, Investigation, Formal analysis, Data curation. **Yuwen Hui:** Writing – original draft, Validation, Data curation. **Junchen Ye:** Writing – review & editing, Validation. **Geng Weng:** Writing – review & editing, Validation. **Ming Li:** Supervision, Software, Resources, Project administration, Funding acquisition, Conceptualization. **Yanhua Wang:** Supervision, Project administration, Funding acquisition, Conceptualization. **Qiaoyi Wu:** Supervision, Project administration, Funding acquisition, Conceptualization.

Funding

This work was supported by the National Key R&D Program of China [grant number 2022YFC3006200], the Natural Science Foundation of China [grant numbers 81901251, 31640045], the Beijing Natural Science Foundation [grant number 7204323, 7232190], the Fujian Provincial Health Technology Project [grant number 2023CXA018] and the Joint Funds for the Innovation of Science and Technology, Fujian Province [grant number 2021Y9107].

Declaration of competing interest

The authors declare that they have no known competing financial interests or personal relationships that could have appeared to influence the work reported in this paper.

Appendix A. Supplementary data

Supplementary data to this article can be found online at https://doi.org/10.1016/j.mtbio.2025.101490.

Data availability

Data will be made available on request.

References

[1] L. Martinengo, M. Olsson, R. Bajpai, M. Soljak, Z. Upton, A. Schmidtchen, J. Car, K. Järbrink, Prevalence of chronic wounds in the general population: systematic review and meta-analysis of observational studies, Ann. Epidemiol. 29 (2019) 8–15.
[2] G.C. Gurtner, S. Werner, Y. Barrandon, M.T. Longaker, Wound repair and regeneration, Nature 453 (2008) 314–321.
[3] L. Su, J. Zheng, Y. Wang, W. Zhang, D. Hu, Emerging progress on the mechanism and technology in wound repair, Biomed. Pharmacother. 117 (2019) 109191.
[4] B.R. Freedman, C. Hwang, S. Talbot, B. Hibler, S. Matoori, D.J. Mooney, Breakthrough treatments for accelerated wound healing, Sci. Adv. 9 (2023) eade7007.
[5] H.N. Wilkinson, M.J. Hardman, Wound healing: cellular mechanisms and pathological outcomes, Open Biol 10 (2020) 200223.
[6] C. Martin-Granados, C.D. McCaig, Harnessing the electric spark of life to cure skin wounds, Adv. Wound Care 3 (2014) 127–138.
[7] R. Luo, J. Dai, J. Zhang, Z. Li, Accelerated skin wound healing by electrical stimulation, Adv. Healthcare Mater. 10 (2021) e2100557.
[8] M. Liu, W. Zhang, S. Han, D. Zhang, X. Zhou, X. Guo, H. Chen, H. Wang, L. Jin, S. Feng, Z. Wei, Multifunctional conductive and electrogenic hydrogel repaired spinal cord injury via immunoregulation and enhancement of neuronal differentiation, Adv Mater 36 (2024) e2313672.
[9] M. Zhao, Electrical fields in wound healing-An overriding signal that directs cell migration, Semin. Cell Dev. Biol. 20 (2009) 674–682.
[10] R.H. Funk, Endogenous electric fields as guiding cue for cell migration, Front. Physiol. 6 (2015) 143.
[11] L. Mao, S. Hu, Y. Gao, L. Wang, W. Zhao, L. Fu, H. Cheng, L. Xia, S. Xie, W. Ye, et al., Biodegradable and electroactive regenerated bacterial cellulose/MXene (Ti(3)C(2)T(x)) composite hydrogel as wound dressing for accelerating skin wound healing under electrical stimulation, Adv. Healthcare Mater. 9 (2020) e2000872.
[12] H. Kai, T. Yamauchi, Y. Ogawa, A. Tsubota, T. Magome, T. Miyake, K. Yamasaki, M. Nishizawa, Accelerated wound healing on skin by electrical stimulation with a bioelectric plaster, Adv. Healthcare Mater. 6 (2017).
[13] R. Dong, P.X. Ma, B. Guo, Conductive biomaterials for muscle tissue engineering, Biomaterials 229 (2020) 119584.
[14] Y. Zhang, M. Li, Y. Wang, F. Han, K. Shen, L. Luo, Y. Li, Y. Jia, J. Zhang, W. Cai, et al., Exosome/metformin-loaded self-healing conductive hydrogel rescues microvascular dysfunction and promotes chronic diabetic wound healing by inhibiting mitochondrial fission, Bioact. Mater. 26 (2023) 323–336.
[15] S.D. Parikh, W. Wang, M.T. Nelson, C.E.W. Sulentic, S.M. Mukhopadhyay, Bioinspired hierarchical carbon structures as potential scaffolds for wound healing and tissue regeneration applications, Nanomaterials 13 (2023).
[16] O. Khrystonko, S. Rimpelová, T. Burianová, V. Švorčík, O. Lyutakov, R. Elashnikov, Smart multi stimuli-responsive electrospun nanofibers for on-demand drug release, J. Colloid Interface Sci. 648 (2023) 338–347.
[17] S.F.C. Guerreiro, J.F.A. Valente, J.R. Dias, N. Alves, Box-behnken design a key tool to achieve optimized PCL/gelatin electrospun mesh, Macromol. Mater. Eng. 306 (2021).
[18] M. Salehi, K. Shahporzadeh, A. Ehterami, H. Yeganehfard, H. Ziaei, M.M. Azizi, S. Farzamfar, A. Tahersoltani, A. Goodarzi, J. Ai, A. Ahmadi, Electrospun poly (ε-caprolactone)/gelatin nanofibrous mat containing selenium as a potential wound dressing material: in vitro and in vivo study, Fibers Polym. 21 (2020) 1713–1721.
[19] N. Wang, W. Liu, G. Chai, S. Sun, Q. Ding, Z. Cheng, X. Liu, Y. Zhao, T. Zhao, Y. Wang, et al., Antibacterial, anti-inflammatory, rapid hemostasis, and accelerated repair by multifunctional metal-organic frameworks fibrous scaffolds for diabetic wounds, Chem. Eng. J. 477 (2023).
[20] S. Qian, J. Wang, Z. Liu, J. Mao, B. Zhao, X. Mao, L. Zhang, L. Cheng, Y. Zhang, X. Sun, W. Cui, Secretory fluid-aggregated janus electrospun short fiber scaffold for wound healing, Small 18 (2022).
[21] A. Enumo Jr., D.F. Argenta, G.C. Bazzo, T. Caon, H.K. Stulzer, A.L. Parize, Development of curcumin-loaded chitosan/pluronic membranes for wound healing applications, Int. J. Biol. Macromol. 163 (2020) 167–179.
[22] S.M. Oliveira, N.M. Alves, J.F. Mano, Cell interactions with superhydrophilic and superhydrophobic surfaces, J. Adhes. Sci. Technol. 28 (2012) 843–863.
[23] D. Cui, M. Li, P. Zhang, F. Rao, W. Huang, C. Wang, W. Guo, T. Wang, Polydopamine-coated polycaprolactone electrospun nanofiber membrane loaded with thrombin for wound hemostasis, Polymers 15 (2023).
[24] Y. Tian, F. Jiang, H. Xie, Z. Chi, C. Liu, Conductive hyaluronic acid/deep eutectic solvent composite hydrogel as a wound dressing for promoting skin burn healing under electrical stimulation, Adv. Healthcare Mater. 13 (2024).
[25] R. Yu, H. Zhang, B. Guo, Conductive biomaterials as bioactive wound dressing for wound healing and skin tissue engineering, Nano-Micro Lett. 14 (2021) 1.
[26] S. Sharma, V.K. Rai, R.K. Narang, T.S. Markandeywar, Collagen-based formulations for wound healing: a literature review, Life Sci. 290 (2022).
[27] J.H. Kim, E.Y. Kim, K.J. Chung, J.H. Lee, H.J. Choi, T.W. Chung, K.J. Kim, Mealworm oil (MWO) enhances wound healing potential through the activation of fibroblast and endothelial cells, Molecules 26 (2021).
[28] K. Scharffetter-Kochanek, C.E. Klein, G. Heinen, C. Mauch, T. Schaefer, B. C. Adelmann-Grill, G. Goerz, N.E. Fusenig, T.M. Krieg, G. Plewig, Migration of a human keratinocyte cell line (HACAT) to interstitial collagen type I is mediated by the alpha 2 beta 1-integrin receptor, J. Invest. Dermatol. 98 (1992) 3–11.
[29] M.S. Criollo-Mendoza, L.A. Contreras-Angulo, N. Leyva-López, E.P. Gutiérrez-Grijalva, L.A. Jiménez-Ortega, J.B. Heredia, Wound healing properties of natural products: mechanisms of action, Molecules 28 (2023).

[30] Y. Hu, S.-S. Rao, Z.-X. Wang, J. Cao, Y.-J. Tan, J. Luo, H.-M. Li, W.-S. Zhang, C.-Y. Chen, H. Xie, Exosomes from human umbilical cord blood accelerate cutaneous wound healing through miR-21-3p-mediated promotion of angiogenesis and fibroblast function, Theranostics 8 (2018) 169–184.
[31] C. Wang, M. Wang, T. Xu, X. Zhang, C. Lin, W. Gao, H. Xu, B. Lei, C. Mao, Engineering bioactive self-healing antibacterial exosomes hydrogel for promoting chronic diabetic wound healing and complete skin regeneration, Theranostics 9 (2019) 65–76.
[32] Y. Hu, R. Tao, L. Chen, Y. Xiong, H. Xue, L. Hu, C. Yan, X. Xie, Z. Lin, A.C. Panayi, et al., Exosomes derived from pioglitazone-pretreated MSCs accelerate diabetic wound healing through enhancing angiogenesis, J. Nanobiotechnol. 19 (2021).
[33] W. Zha, J. Wang, Z. Guo, Y. Zhang, Y. Wang, S. Dong, C. Liu, H. Xing, X. Li, Efficient delivery of VEGF-A mRNA for promoting diabetic wound healing via ionizable lipid nanoparticles, Int J Pharm 632 (2023) 122565.
[34] J. Wang, J. Lin, L. Chen, L. Deng, W. Cui, Endogenous electric-field-coupled electrospun short fiber via collecting wound exudation, Adv. Mater. 34 (2022).
[35] K. Raziyeva, Y. Kim, Z. Zharkinbekov, K. Kassymbek, S. Jimi, A. Saparov, Immunology of acute and chronic wound healing, Biomolecules 11 (2021).
[36] Y. Xiong, B.-B. Mi, Z. Lin, Y.-Q. Hu, L. Yu, K.-K. Zha, A.C. Panayi, T. Yu, L. Chen, Z.-P. Liu, et al., The role of the immune microenvironment in bone, cartilage, and soft tissue regeneration: from mechanism to therapeutic opportunity, Military Medical Research 9 (2022).
[37] Q. Wang, H. Wang, Y. Ma, X. Cao, H. Gao, Effects of electroactive materials on nerve cell behaviors and applications in peripheral nerve repair, Biomater. Sci. 10 (2022) 6061–6076.
[38] J. Sun, W. Xie, Y. Wu, Z. Li, Y. Li, Accelerated bone healing via electrical stimulation, Adv. Sci. (2024) e2404190.
[39] H. Yao, X. Yuan, Z. Wu, S. Park, W. Zhang, H. Chong, L. Lin, Y. Piao, Fabrication and performance evaluation of gelatin/sodium alginate hydrogel-based macrophage and MSC cell-encapsulated paracrine system with potential application in wound healing, Int. J. Mol. Sci. 24 (2023).
[40] Y. Long, H. Wei, J. Li, G. Yao, B. Yu, D. Ni, A.L.F. Gibson, X. Lan, Y. Jiang, W. Cai, X. Wang, Effective wound healing enabled by discrete alternative electric fields from wearable nanogenerators, ACS Nano 12 (2018) 12533–12540.
[41] A.P. Veith, K. Henderson, A. Spencer, A.D. Sligar, A.B. Baker, Therapeutic strategies for enhancing angiogenesis in wound healing, Adv. Drug Deliv. Rev. 146 (2019) 97–125.